Journal of ELECTRONIC MATERIALS, Vol. 41, No. 6, 2012
DOI: 10.1007/s11664-011-1875-7

In Situ Growth of a Yb_2O_3 Layer for Sublimation Suppression for $Yb_{14}MnSb_{11}$ Thermoelectric Material for Space Power Applications

JAMES A. NESBITT,[1,3] ELIZABETH J. OPILA,[2] and MICHAEL V. NATHAL[1]

1.—NASA Glenn Research Center, Cleveland, OH 44135, USA. 2.—University of Virginia, Charlottesville, VA 22904, USA. 3.—e-mail: JNesbitt@NASA.gov

The compound $Yb_{14}MnSb_{11}$ is a *p*-type thermoelectric material of interest to the National Aeronautics and Space Administration (NASA) as a candidate replacement for the state-of-the-art Si-Ge used in current radioisotope thermoelectric generators (RTGs). Ideally, the hot end of this leg would operate at 1000°C in the vacuum of space. Although $Yb_{14}MnSb_{11}$ shows the potential to double the value of the thermoelectric figure of merit (zT) over that of Si-Ge at 1000°C, it suffers from a high sublimation rate at elevated temperatures and would require a coating in order to survive the required RTG lifetime of 14 years. The purpose of the present work is to measure the sublimation rate of $Yb_{14}MnSb_{11}$ and to investigate sublimation suppression for this material. This paper reports on the sublimation rate of $Yb_{14}MnSb_{11}$ at 1000°C ($\sim 3 \times 10^{-3}$ g/cm^2 h) and efforts to reduce the sublimation rate with an *in situ* grown Yb_2O_3 layer. Despite the success in forming thin, dense, continuous, and adherent oxide scales on $Yb_{14}MnSb_{11}$, the scales did not prove to be sublimation barriers.

Key words: Zintl, $Yb_{14}MnSb_{11}$, sublimation, coatings, oxidation

INTRODUCTION

The compound $Yb_{14}MnSb_{11}$ is a *p*-type thermoelectric (TE) material[1] of interest to National Aeronautics and Space Administration (NASA) as a candidate replacement for the state-of-the-art Si-Ge used in current radioisotope thermoelectric generators (RTGs). $Yb_{14}MnSb_{11}$ shows the potential to double the value of the thermoelectric figure of merit (zT) over that of Si-Ge at 1000°C[1,2] and has received significant attention in recent years.[1–4] However, the sublimation rate of $Yb_{14}MnSb_{11}$ at 1000°C could be problematic. The calculated vapor pressures at 1000°C for pure Yb and Sb are 2.2×10^{-1} atm and 2.8×10^{-1} atm, respectively, whereas in comparison, the vapor pressures for pure Si and Ge are 0.18×10^{-10} atm and 5.0×10^{-10} atm.[5] The vapor pressure for pure Mn is intermediate to Ge and Sb at 2.4×10^{-5} atm.[5] [Where more than one vapor species is predicted (e.g., Sb_2, Sb_3, Sb_4), the sum of the pressures for all species of that element is given.] Although unit activities have been assumed in these calculations and the actual activity of each element in the compound could be significantly lower, these calculations indicate the potential for high vapor pressures for Yb-Mn-Sb compounds. Since the sublimation rate is proportional to the vapor pressure according to the Hertz–Knudsen–Langmuir equation,[6] the high vapor pressures of the pure elements suggest the possibility of a high sublimation rate for the compound. Since Si-Ge alloys require a thin Si_3N_4 coating to suppress sublimation, primarily of the Ge,[7] $Yb_{14}MnSb_{11}$ could require even greater sublimation suppression at 1000°C.

Based on shrinking TE leg cross-sections, researchers at NASA's Jet Propulsion Lab (JPL) set the maximum acceptable sublimation rate for $Yb_{14}MnSb_{11}$ at approximately 1×10^{-6} g/cm^2 h in order to meet power goals for a 14-year lifetime.[8]

(Received July 15, 2011; accepted December 16, 2011; published online February 7, 2012)

However, early testing at JPL[9,10] indicated that the sublimation rate of $Yb_{14}MnSb_{11}$ at 1000°C in vacuum was $\sim 1 \times 10^{-3}$ g/cm^2 h. Hence, a coating would be required to reduce the sublimation rate of $Yb_{14}MnSb_{11}$ by approximately three orders of magnitude for use at 1000°C. The first purpose of this study is to confirm the sublimation rate of uncoated $Yb_{14}MnSb_{11}$.

One of the simplest coatings, whether for sublimation or oxidation protection, is to selectively oxidize a component in an alloy to form an oxide layer. This process is used routinely for protection of gas-turbine components in aero engines operating in oxidizing environments.[11,12] Thin Al_2O_3, and sometimes Cr_2O_3 or SiO_2 layers grow on the surface to reduce the oxidation rate and thereby protect the component. Qualities of a protective oxide scale are that it must be slow growing, fully cover the surface, and be adherent, especially in applications where thermal cycling occurs, which tends to crack or spall the oxide layer due to thermal expansion mismatch. Since the oxide scale is grown on the surface, it is thermodynamically stable with the substrate when maintained at the same temperature (i.e., it does not react or form other compounds, although an oxide layer may continue to grow thicker with time in the presence of oxygen). The second purpose of this study is to examine thin, *in situ* oxide coatings for sublimation suppression. Results with thin metallic and oxide coatings will be presented in a future paper.

EXPERIMENTAL PROCEDURES

$Yb_{14}MnSb_{11}$ was fabricated at JPL by hot pressing ball-milled powders.[10] Short rods (ϕ = 12 mm) of $Yb_{14}MnSb_{11}$ were provided by JPL to the NASA Glenn Research Center (GRC) for evaluation. These rods were sectioned into thin disks approximately 1.5 mm thick. The faces and edges of the disks were polished through 4000 grit SiC paper. To extend the limited supply of material, these disks were cut into quarters. All samples were cleaned in acetone and ethanol before testing. The surface area and weight of the $Yb_{14}MnSb_{11}$ samples were measured before each test. The weight loss divided by the exposure time and exposed surface area provided the sublimation rate. Since each piece was hand cut and polished, the accuracy of the surface area measurements ($\sim X$ cm^2), and therefore the sublimation rates, is estimated at ±10%. The quarter disk $Yb_{14}MnSb_{11}$ samples were laid flat in a high-purity alumina boat. Furnace testing at 1000°C (±2°C) was performed in a horizontal tube furnace for 24 h to 168 h using two test configurations.

Initially, $Yb_{14}MnSb_{11}$ samples were encapsulated in long, evacuated, and sealed quartz tubes to enable a continuous cycle of sublimation from the hot sample and condensation onto the cool sections of the quartz tube during the test (static vacuum test). The quartz tube was approximately 2.5 cm outer diameter (OD) and 76 cm to 101 cm long. To prevent the Yb vapor from reacting with and reducing the SiO_2 in the quartz tubes, an inner, closed-end alumina tube was placed as an inner sleeve inside the quartz tube. The quartz tube with the samples was evacuated to pressure of typically 5×10^{-4} Pa to 8×10^{-4} Pa (4×10^{-6} Torr to 6×10^{-6} Torr) prior to sealing. In a second configuration, the closed-end quartz tube extending into the horizontal furnace remained connected with a continuously running turbopump (dynamic vacuum test). Again, the sublimate deposited on the cool walls of the tube extending outside of the furnace. For most of the dynamic vacuum tests, larger 5.0-cm-OD closed-end quartz tubes were used with 3.4-cm-OD closed-end, inner alumina tubes. After an initial deterioration in the vacuum during heating, pressures in the tube during the dynamic vacuum tests were similar to those for the static vacuum tests.

Tests in both configurations were performed both with and without a coiled Zr foil to act as an oxygen getter. The coiled Zr foil was placed in the alumina tube approximately 1 cm from the alumina boat holding the $Yb_{14}MnSb_{11}$ samples. Since the vapor pressure of pure Zr at 1000°C is more than 16 orders of magnitude less than that of Yb or Sb,[5] it was not expected that any Zr would sublime or react in any way with the $Yb_{14}MnSb_{11}$ material. As expected, after testing, no Zr was ever found on the $Yb_{14}MnSb_{11}$ samples, although Sb vapor was found to have deposited and reacted with the Zr foil.

Following testing, any oxide which formed on the surface of the samples was removed prior to weighing. All oxide encountered was loosely attached and easily removed by lightly brushing or using clean compressed air. X-ray diffraction was performed on this oxide and on the sample surface. After x-ray diffraction, samples were sectioned, vacuum mounted in epoxy, and polished. The polished cross-sections were examined optically, by scanning electron microscopy (SEM), and with energy-dispersive spectroscopy (EDS).

To evaluate *in situ* formed oxide coatings as sublimation barriers, oxide layers were grown on quarter disk samples in a horizontal tube furnace in either air or flowing Ar-5%H_2. Sample surfaces were polished as for previous sublimation testing. The samples were laid flat in a high-purity alumina boat during oxidation. After it was found that oxidation in static air at 400°C yielded unacceptable thick, cracked, and spall-prone scales, subsequent oxidation producing thin, adherent scales was performed in flowing Ar-5%H_2 (100 sccm) at 350°C to 450°C for 2 h to 16 h. Following the growth of the oxide layer, the samples were evaluated in the dynamic vacuum test with Zr foil, as previously described.

RESULTS AND DISCUSSION

Sublimation Rates of Uncoated $Yb_{14}MnSb_{11}$

The measured sublimation rates varied from 0.3×10^{-3} g/cm^2 h to 3×10^{-3} g/cm^2 h, as shown in

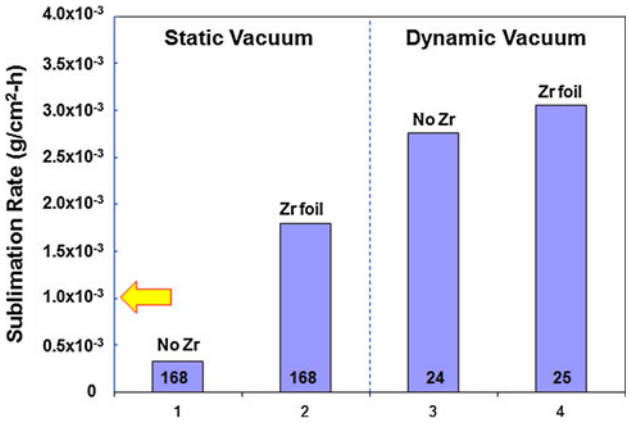

Fig. 1. Sublimation rates for uncoated $Yb_{14}MnSb_{11}$ samples tested at 1000°C. The numbers within each bar indicate the duration (h) of the test. Arrow indicates rate measured by JPL.[10]

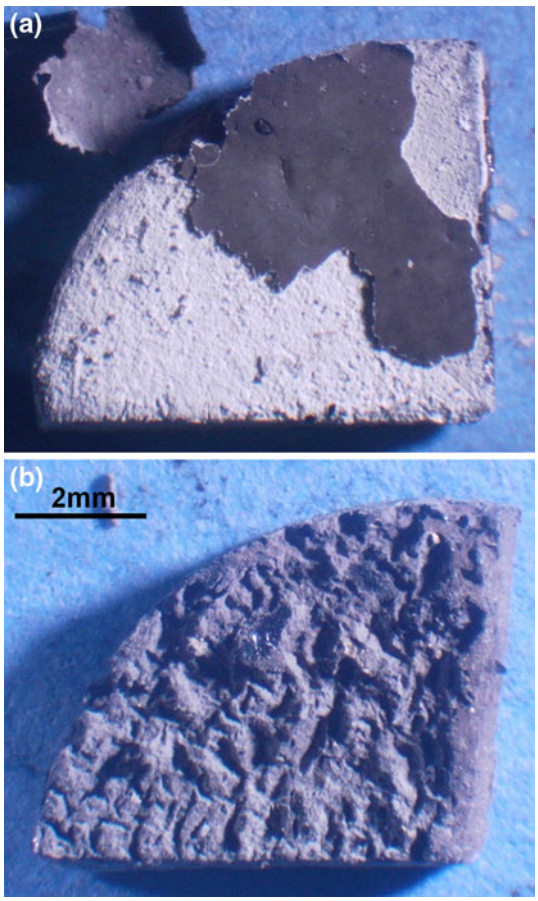

Fig. 2. Uncoated $Yb_{14}MnSb_{11}$ after static vacuum testing for 168 h (a) without Zr foil, and (b) with Zr foil. In (b), a thin layer of white, powdery Yb_2O_3 oxide has been removed.

Fig. 1. These rates were in general agreement with that reported by JPL ($\sim 1 \times 10^{-3}$ g/cm^2 h).[10] For the static vacuum tests, the test which included the Zr foil showed a significantly higher sublimation rate

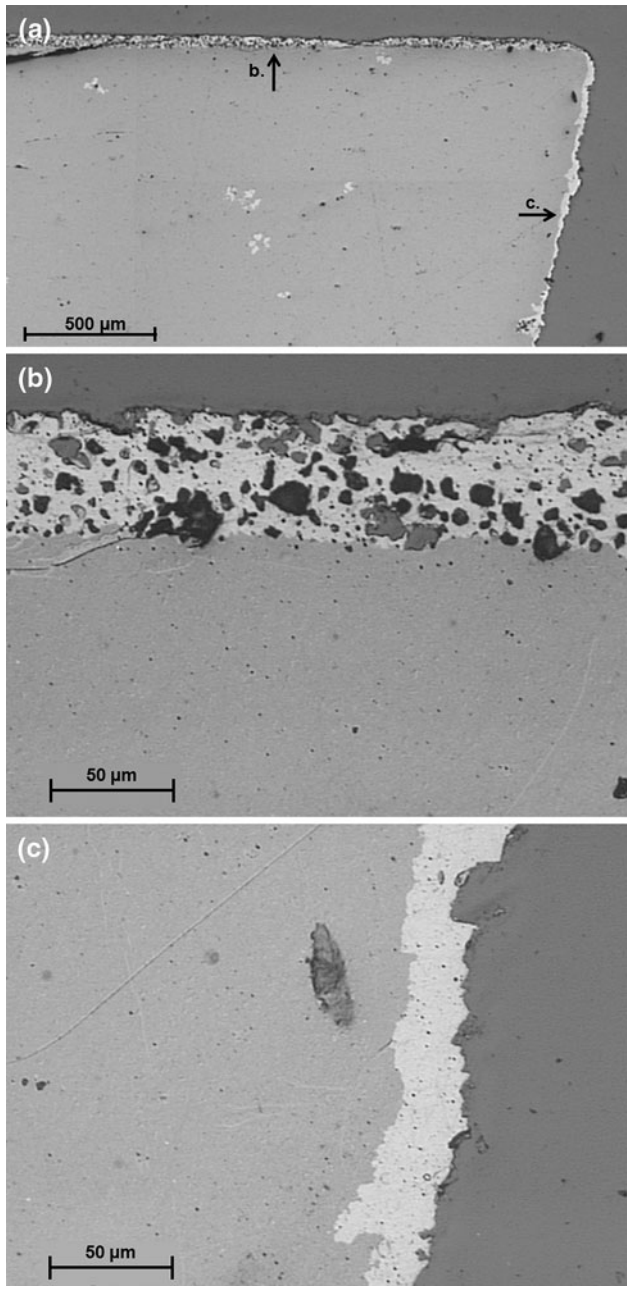

Fig. 3. Optical micrographs of (a) polished cross-section of the sample from the static vacuum test without Zr foil for 168 h at 1000°C (see Fig. 2a). (b) Magnified view of the top surface and (c) side surface as indicated in (a).

(1.8×10^{-3}) than for that without the foil (0.3×10^{-3} g/cm^2 h). For the dynamic vacuum tests, the rate was only slightly higher with than without the Zr foil (3×10^{-3} g/cm^2 h versus 2.8×10^{-3} g/cm^2 h).

After testing, all of the samples had some white, powdery oxide on the surface, which was identified by x-ray diffraction as Yb_2O_3. Samples after 168 h in the static vacuum test are shown in Fig. 2. The sample without Zr foil had the most surface oxide,

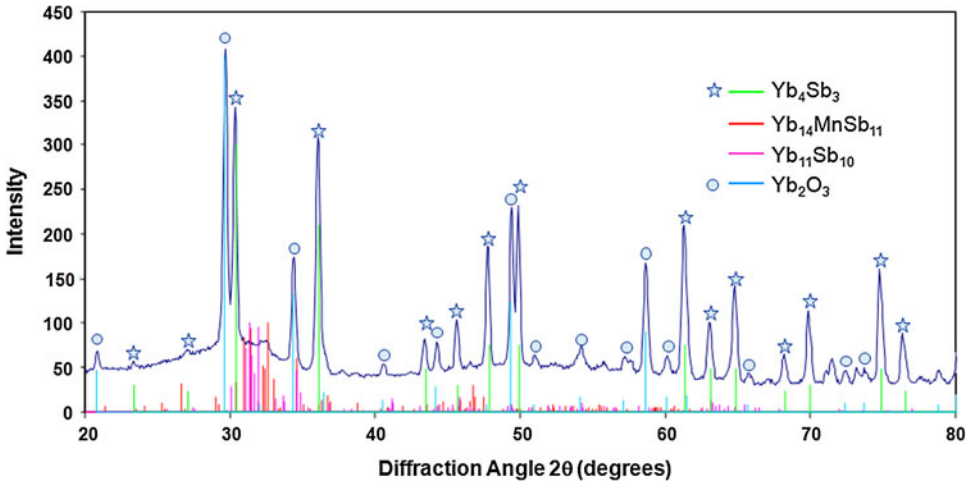

Fig. 4. X-ray diffraction scan from the surface of the sample shown in Fig. 3 (static vacuum, without Zr foil) after removal of most of the oxide. All major peaks are in good agreement with either Yb_2O_3 or Yb_4Sb_3.

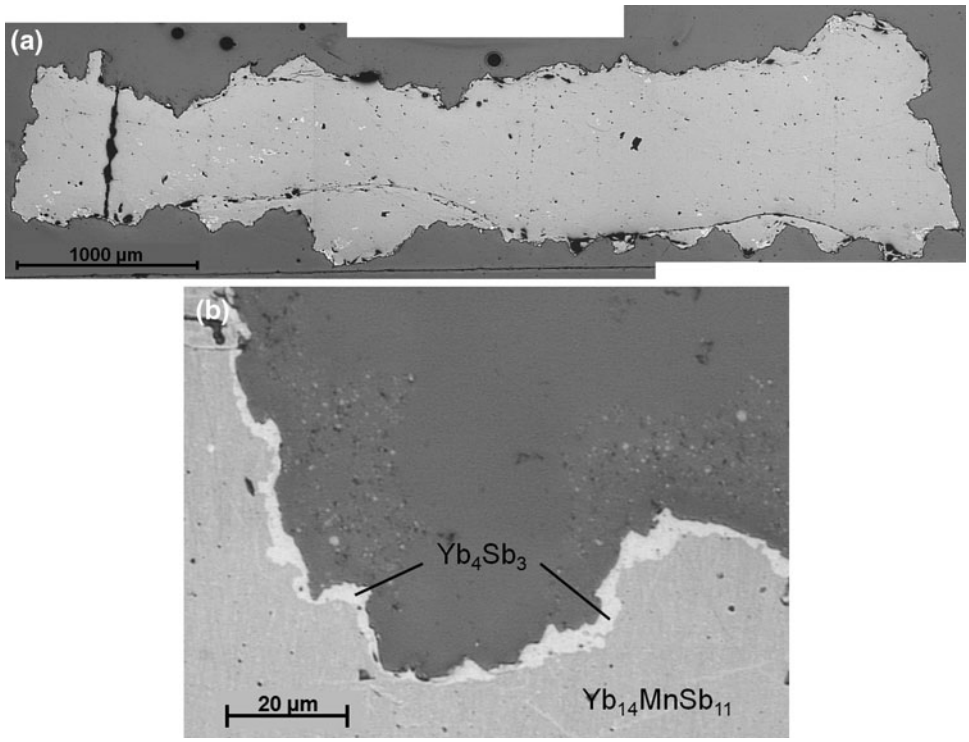

Fig. 5. (a) Optical micrographs of polished cross-section of the encapsulated sample tested in vacuum with the Zr foil for 168 h at 1000°C. (b) Optical micrograph of the near-surface region showing the thin Yb_4Sb_3 phase.

which included a dark, detached oxide layer above the white, powdery Yb_2O_3 (Fig. 2a). X-ray diffraction of both sides of this dark scale also indicated Yb_2O_3. Not surprisingly, this sample with the thickest oxide layer exhibited the lowest sublimation rate. Significant surface deformation associated with the loss of material was evident for the sample with the Zr foil which exhibited the higher sublimation rate (Fig. 2b).

The polished cross-section of the static vacuum sample tested without Zr foil (Fig. 2a) is shown in Fig. 3. Most obvious is the presence of a near-surface phase (Fig. 3b, c). X-ray diffraction of the sample surface identified this layer as Yb_4Sb_3 (Fig. 4) with all other major peaks associated with Yb_2O_3. On the top surface, this Yb_4Sb_3 layer was relatively thick (~50 μm) and contained numerous pores, many of which were filled with epoxy,

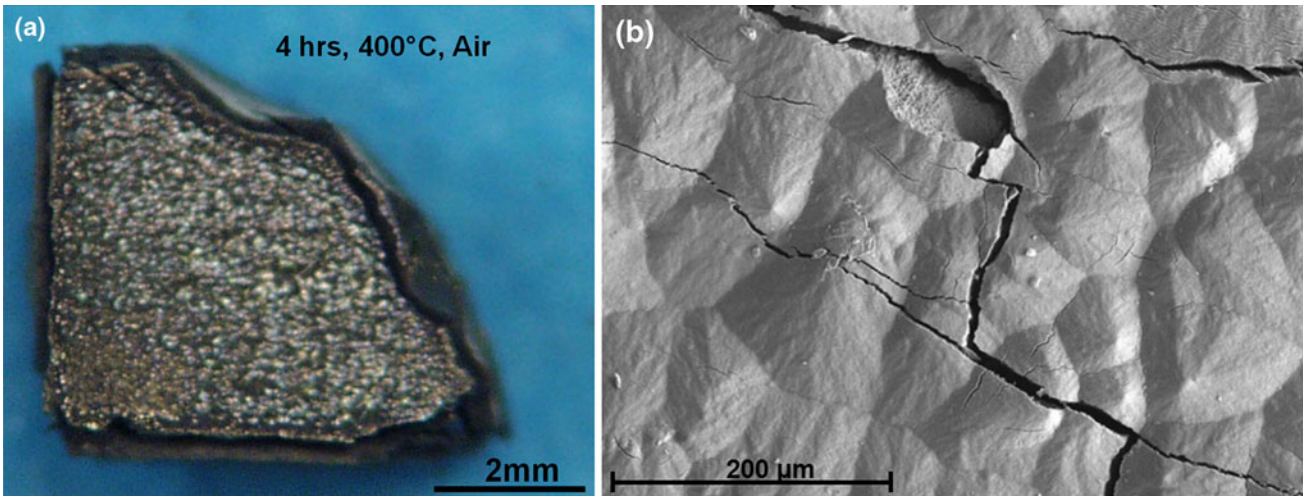

Fig. 6. $Yb_{14}MnSb_{11}$ sample oxidized for 4 h in air at 400°C. (a) Macro photo showing thick oxide scale on edges, (b) SEM micrograph of the oxide on the polished surface showing a thick, cracked oxide layer.

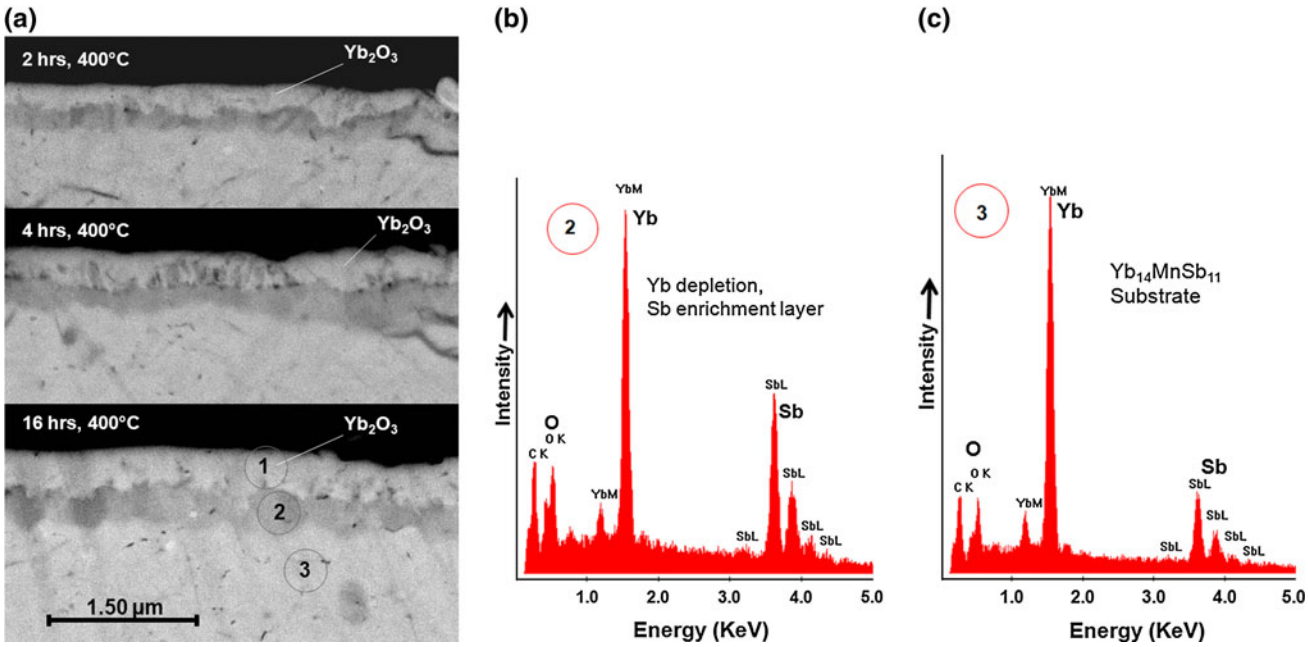

Fig. 7. (a) SEM back-scattered electron (BSE) micrographs of $Yb_{14}MnSb_{11}$ samples oxidized in Ar-5%H_2 at 400°C for the indicated times, (b, c) spectra taken at points 2 and 3 indicated in the 16 h image.

indicating open connectivity with the surface (Fig. 3b). However, on the side of the sample, the Yb_4Sb_3 layer was about half as thick and without pores (Fig. 3c).

The polished cross-section of the static vacuum sample tested with Zr foil (Fig. 2b) is shown in Fig. 5. A thinner, near-surface layer of Yb_4Sb_3 was evident on this sample (Fig. 5b) as well as on the surface of the samples with the higher sublimation rates tested in the dynamic vacuum tests. Porosity in the thinner layer was only occasionally observed. If the Mn concentration is ignored, the formation of the Yb_4Sb_3 phase suggests that the surface is becoming slightly enriched in Yb or depleted in Sb since the Yb/Sb molar ratio for $Yb_{14}Sb_{11}$ is 1.27 while that for Yb_4Sb_3 is 1.33. (Identical results are derived when examining Yb/Sb ratios using mass fractions or wt%.) Hence, if the Mn can be ignored, the formation of the Yb_4Sb_3 phase suggests Sb is subliming at a slightly higher rate than the Yb. However, oxygen was also detected by EDS in the as-received $Yb_{14}MnSb_{11}$ material prior to testing, indicating a relatively high solubility. It is possible that either an elevated or depleted level of oxygen near the surface could also have helped stabilize the Yb_4Sb_3 phase.

It is obvious from Fig. 5 that massive material loss has occurred after only 168 h with the relatively high sublimation rate ($\sim 2 \times 10^{-3}$ g/cm^2 h). The initial thickness of this sample was 0.205 cm (2050 μm). Most of the remaining cross-section is approximately half or less of that original thickness. This high material loss demonstrates not only the need for a good sublimation suppression coating, but also that the coating must be nearly defect free without cracks or pin holes that would allow the $Yb_{14}MnSb_{11}$ vapor to escape.

It appears likely that the thicker layer of oxide formed on the surface of the sample from the static vacuum test without the Zr foil was the cause for the lower sublimation rate of that sample. It is possible that the higher sublimation rates observed with the three other samples, which resulted in more rapid metal loss and higher surface recession rates, also resulted in the thinner Yb_4Sb_3 layer. Similarly, the lower sublimation rate, and lower surface recession resulted in the thicker Yb_4Sb_3 layer. The pores in this layer have the appearance of a type of Kirkendall porosity which forms as the result of unequal intrinsic diffusive fluxes.[13,14] In this scenario, unequal flows of Yb and Sb towards, and Mn away from, the receding surface result in excess vacancies in the Yb_4Sb_3 layer which can coalesce into pores. The presence of the pores in certain regions but not others is not understood but could be a function of the sublimation rate, thickness of any surface oxide, and amount of vacancy sources and sinks in the metal.

In Situ Growth of a Yb_2O_3 Layer for Sublimation Suppression

A dense Yb_2O_3 scale was intentionally grown on the surface of the $Yb_{14}MnSb_{11}$ as a sublimation suppression layer. The free energy of formation of Yb_2O_3 is much lower (more negative) than that for the oxides of either Mn or Sb,[5] making it possible to selectively oxidize the Yb to form a Yb_2O_3 layer. This layer would have the benefit of thermodynamic stability with the substrate. However, this oxide layer would have to be more protective than the powdery Yb_2O_3 previously found on the sample surface after sublimation testing at 1000°C. The first oxidation exposure for 4 h at 400°C in air resulted in a thick, cracked, nonadherent oxide scale, as shown in Fig. 6. The extent of oxidation was decreased by oxidizing in flowing Ar-5%H_2 at 350°C for 16 h, at 400°C for 2 h, 4 h, and 16 h, and at 450°C for 2 h. Although no oxidation is predicted in the Ar-5%H_2 environment, there was sufficient oxygen present in the furnace system to form thin, transparent, adherent scales in all cases. The source of the oxygen was possibly water vapor adsorbed on the furnace tube walls. It is likely that the scales were amorphous, although this could not be determined with certainty because of the scale thickness.

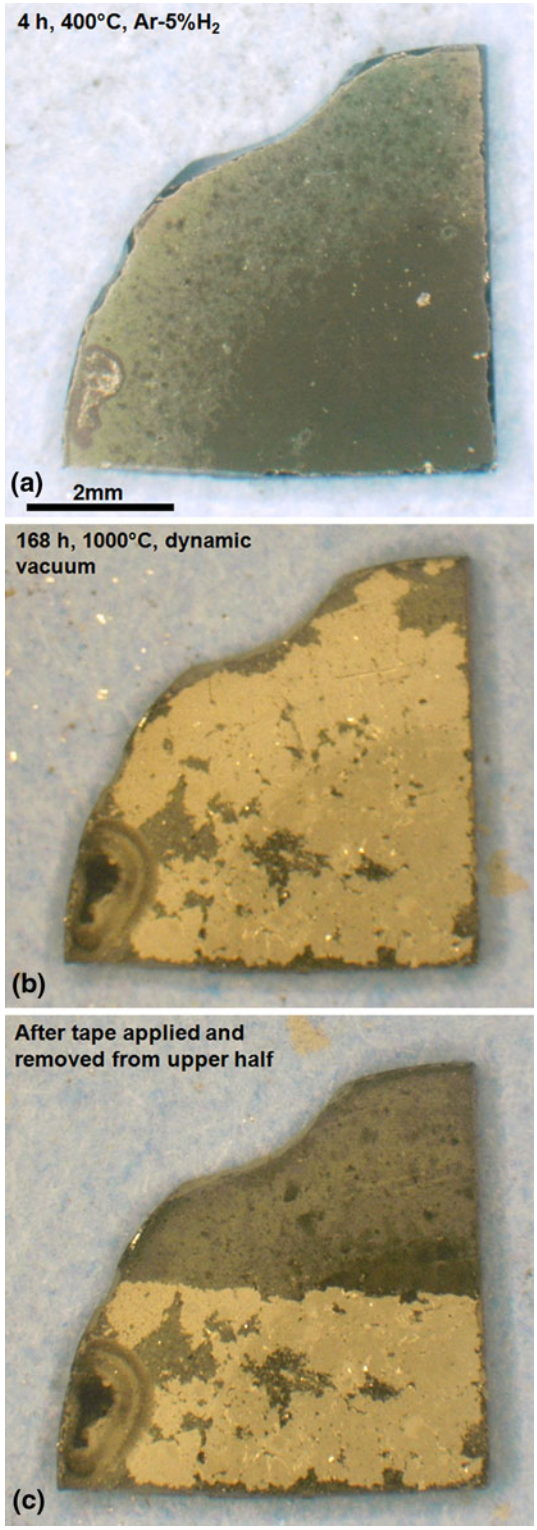

Fig. 8. Optical macrographs of a $Yb_{14}MnSb_{11}$ sample oxidized in Ar-5%H_2 at 400°C for 4 h (a) before, and (b) after sublimation testing in a dynamic vacuum for 168 h at 1000°C, and (c) after tape-pull test of oxide on the upper half of the sample.

Cross-sectional views of the oxide shown after oxidation in Ar-5%H_2 for 2 h, 4 h, and 16 h at 400°C are shown in Fig. 7. Two layers are evident: a

thinner, light-shaded outer layer (designated 1 in the 16 h sample) and a thicker, dark inner layer (designated 2). EDS analysis showed the outer layer (1) to be the expected Yb_2O_3. Comparison of the EDS spectra of the dark inner layer (Fig. 7b) with the $Yb_{14}MnSb_{11}$ substrate (designated 3) shows the dark layer to be enriched in Sb but also higher in oxygen, suggesting that this layer could be a transient mixed oxide of Yb and Sb. The approximate thicknesses for the outer Yb_2O_3 layer were 0.2 μm after 2 h, 0.3 μm after 4 h, and 0.4 μm after 16 h. This indicates subparabolic growth of the oxide layer and could be related to a fixed quantity of available oxygen in the furnace tube.

The oxidized samples were sublimation tested in a dynamic vacuum for 168 h at 1000°C with the Zr foil as an oxygen getter. After this testing, the oxide scale became relatively opaque, friable, and detached from the sample. The initial, transparent nature of the oxide is indicated in the image of the sample after oxidation but before testing in Fig. 8a. The lighter color of the opaque scale after testing is evident in Fig. 8b. The poor adhesion of the scale was demonstrated by applying and removing a piece of tape on the surface (Fig. 8c). Under this loose oxide layer, the $Yb_{14}MnSb_{11}$ surface was rough, indicating that significant sublimation had occurred. Cross-sectional examination of the near-surface region showed the rough surface with small pits as well as the presence of the near-surface Yb_4Sb_3 layer, features indicating material loss by sublimation. It appears that the thin scale crystallized at the test temperature and became friable, with little bond to the surface, similar to the powdery Yb_2O_3 which formed on the surface during testing of uncoated $Yb_{14}MnSb_{11}$. Consequently, thermally grown *in situ* Yb_2O_3 layers, grown at low temperatures and at low oxygen pressures, although thin and adherent before testing, were not adherent or effective as sublimation barriers for $Yb_{14}MnSb_{11}$ at 1000°C.

CONCLUSIONS

The sublimation rate of uncoated $Yb_{14}MnSb_{11}$ was measured to be as high as 3×10^{-3} g/cm^2 h in vacuum at 1000°C. While testing at 1000°C and pressures of 5×10^{-4} Pa to 8×10^{-4} Pa (4×10^{-6} Torr to 6×10^{-6} Torr), with or without Zr foil as an oxygen getter, Yb_2O_3 formed on the surface of the $Yb_{14}MnSb_{11}$ as a thin, white, powdery layer. Heavy formation of this oxide in a static vacuum without the Zr foil appeared to reduce the sublimation rate by about 8× over a light formation of the oxide after testing in a dynamic vacuum with Zr foil. For sublimation suppression, a thin, dense, adherent layer of Yb_2O_3 was grown on the $Yb_{14}MnSb_{11}$ at low temperatures and low oxygen pressures. However, this thin layer likely crystallized and became friable at the higher test temperature, debonded from the surface, and offered little protection against sublimation. Additional work with various metallic and ceramic coatings for sublimation suppression has been performed and will be reported in the future.

ACKNOWLEDGEMENTS

The support of the Radioisotope Power Systems office at the NASA Glenn Research Center is gratefully acknowledged.

REFERENCES

1. S.R. Brown, S.M. Kauzlarich, F. Gascoin, and G.J. Snyder, *Chem. Mater.* 18, 7 (2006).
2. S.R. Brown, E.S. Toberer, T. Ikeda, C.A. Cox, F. Gascoin, S.M. Kauzlarich, and G.J. Snyder, *Chem. Mater.* 20, 10 (2008).
3. C. Cox, S. Brown, G. Snyder, and S. Kauzlarich, *J. Electron. Mater.* 39, 9 (2010).
4. E.S. Toberer, S.R. Brown, T. Ikeda, S.M. Kauzlarich, and G.J. Snyder, *Appl. Phys. Lett.* 93, 062110 (2008).
5. C.W. Bale, E. Bélisle, P. Chartrand, S.A. Decterov, G. Eriksson, K. Hack, I.H. Jung, Y.B. Kang, J. Melançon, A.D. Pelton, C. Robelin, and S. Petersen, *Comput. Coupl. Phase Diagr. Thermochem.* 33, 295 (2009).
6. J.H. Jeans, *An Introduction to the Kinetic Theory of Gases* (London: Cambridge University Press, 1962).
7. M.S. El-Genk, H.H. Saber, T. Caillat, and J. Sakamoto, *Energy Convers. Manag.* 47, 174 (2006).
8. T. Caillat, in *Quarterly Management Review (MMR), Power & ISRU Technology Programs—SMD, October–December 2007* (NASA-Jet Propulsion Laboratory, Pasadena, 2008, unpublished).
9. J. Sakamoto, *Technical Review, Power & ISRU Technology Programs SMD* (NASA-Jet Propulsion Laboratory, Pasadena, 2006, unpublished).
10. R. Ewell, T. Caillat, *Advanced Thermoelectric Converter (ATEC) Annual Report (January 2006–January 2007)* (NASA-Jet Propulsion Laboratory, California Institute of Technology, Pasadena, CA, 2007, unpublished).
11. N. Birks, G. Meier, and F. Pettit, *Introduction to the High Temperature Oxidation of Metals*, 2nd ed. (Cambridge University Press: Cambridge, 2006).
12. J. Smialek and G. Meier, *Superalloys II—High Temperature Materials for Aerospace and Industrial Power* (New York: Wiley-Interscience, John Wiley and Sons, 1987), p. 293.
13. J. Philibert, *Atom Movements: Diffusion and Mass Transport in Solids* (Monographies de Physique) (Les Editions de Physique, 1991).
14. H. Strandlund and H. Larsson, *Acta Mater.* 52, 4695 (2004).